



OPEN A study on the miscibility mechanisms and patterns of high CO₂ content associated gas reinjection

Yunfei Lei^{1,2}, Changquan Wang^{1,2}✉, Shijing Xu^{1,2}, Lihong Shi^{1,2}, Xinke Jin^{1,2} & Weijie Fu^{1,2}

To investigate the enhanced oil recovery mechanisms during the reinjection of CO₂-rich associated gas, analyse the miscibility behaviour between associated gas and crude oil, and provide guidance for increasing oil recovery in field development, in this study, gas injection expansion experiments, solubility measurements of various gases in crude oil, and slim tube experiments were conducted. The experimental results demonstrated that CH₄ and N₂ could reduce the solubility of associated gas in crude oil. The solubility of associated gas without CH₄ and N₂ in crude oil was 1.05 to 3.22 times greater than that of CO₂, whereas their removal enabled the solubility of associated gas in crude oil to surpass that of CO₂. Both CO₂ and associated gas could cause crude oil to swell and reduce its viscosity, and the absence of CH₄ and N₂ amplified these effects. The minimum miscibility pressure (MMP) for CO₂ flooding is 24.29 MPa, while a reservoir pressure of 21 MPa is insufficient to achieve miscible flooding. Removing CH₄ and N₂ from the associated gas can reduce the MMP by up to 48%, resulting in a 25.59% increase in the oil recovery efficiency.

Abbreviations

BPV	Back pressure valve
CCUS	Carbon capture, utilization, and storage
CCE	Constant-composition expansion
EOR	Enhance oil recovery
EC	Expansion coefficient
GOR	Gas–oil ratio
HSE	Health, safety, and environmental
MMP	Minimum miscibility pressure
MMcfd	Millions of cubic feet per day
P _b	Bubble point pressure
P–V	Pressure–volume
PV	Pore volume

Within the context of the dual carbon era, carbon capture, utilization, and storage (CCUS) has become a key focus. Currently, the use of CO₂ flooding technology for oil recovery has become increasingly mature in various oilfields.

During reservoir exploitation, oil wells produce both crude oil and associated gas. Owing to the high reservoir heterogeneity resulting from the sedimentary environments in China and the issue of CO₂ gas breakthrough at the later stages of development, the CO₂ content in associated gas has increased sharply. This restricts the efficient utilization of CO₂ and its effective sequestration in reservoirs^{1–3}. After crude oil extraction, the oil and gas enter the metering station through the oil pipeline. Following processing through a buffer tank, separator, booster pump, and other equipment, the CO₂ content in the associated gas increases further^{4–6}. The combustion of associated gas with a high CO₂ content cannot meet the required calorific value. Purifying CO₂ through physical or chemical adsorption methods for further use increases costs, adds complexity to the process, and reduces the production efficiency^{7–9}. However, directly reinjecting such high-CO₂-content associated gas into the reservoir for enhanced oil recovery can provide both economic benefits and environmental compliance.

¹State Key Laboratory of Low Carbon Catalysis and Carbon Dioxide Utilization, Yangtze University, Wuhan 430100, China. ²Key Laboratory of Drilling and Production Engineering for Oil and Gas, Yangtze University, Wuhan 430100, China. ✉email: 500912@yangtzeu.edu.cn

The Weyburn Oilfield in Canada is the largest CO₂ flooding demonstration project to date. Since 2000, 1 million tons of CO₂ has been injected annually for enhanced oil recovery purposes. In 2010, the oilfield began researching associated gas reinjection, and currently, reinjected CO₂ accounts for 50% of the total injection volume^{10,11}. In recent years, there has been a significant amount of research on associated gas reinjection¹²; for example, Kun Su et al.¹³ employed numerical simulation methods to study the effect of direct associated gas reinjection in the Jilin Oilfield and reported that it could increase oil recovery. Yang et al.¹⁴ conducted a full-component analysis of crude oil produced at different stages and reported that the proportion of each component in the produced oil before gas breakthrough was similar to that in the initial crude oil. After gas breakthrough, the proportion of light components in the produced oil gradually increased. When the CO₂ concentration in the reinjected gas was less than 25%, the changes in the components of the produced crude oil were not significant.

Rich gas, which is an important component of associated gas, contributes to enhanced oil recovery¹⁵. The United States and Canada were among the first to conduct field trials in which rich gas was injected to increase oil recovery^{16–18}. In the former Soviet Union, the alternating water–gas injection technique was successfully applied in the North Sea Oilfield^{19,20}. In Venezuela, the once largest natural gas injection project for enhanced oil recovery in the world was implemented²¹. As early as the 1980s, Chen et al.²² studied the impact of the solvent slug size on the oil recovery efficiency during rich gas miscible flooding and established a slug size calculation model considering multiple factors. GLASO²³ proposed a relationship equation for predicting the minimum miscibility pressure (MMP) between rich gas and crude oil. SHYEH-YUNG²⁴ studied the impacts of the components of enriched gas and injection pressure on the displacement efficiency. Regarding the reinjection of enriched associated gas, Hoffman et al.²⁵ investigated gas injection for enhanced oil recovery in the Elm Coulee shale reservoir under both miscible and immiscible conditions using numerical simulations. Their comparison revealed that rich gas injection could increase the recovery factor. Tao Wan et al.²⁶ focused on the Eagle Ford Shale as their study subject, accounting for uncertainties in oil composition changes. They developed a geological model using a stable black oil model and, on the basis of this model, employed commercial simulation software to simulate cyclic rich gas injection, thereby optimizing the injection strategy to increase the recovery factor. Morteza Akbarabadi²⁷ demonstrated, through core displacement experiments, that hydrocarbon gases coproduced with crude oil play a significant role in enhancing oil recovery. Ala Eddine Aoun et al.²⁸ on the basis of the field conditions of the Bakken Reservoir, proposed an alternating injection scheme of associated gas with a rate of 3 MMcf/d, thereby considering capital expenditure, operational costs, and oil revenue. Their calculations indicated that this approach could increase oil production by 70%²⁹. Progress has also been reported in recent years in many other oilfields worldwide^{30–32}.

The H block of the Jilin Oilfield exhibits a reservoir depth of 2450 m, porosities ranging from 8 to 15%, and high heterogeneity. To maintain the reservoir pressure and well productivity, CO₂ injection was initially employed, followed by water injection at the later stages of reservoir development. Currently, the H block occurs in the late phase of gas injection, with a reservoir pressure of 21 MPa, a reservoir temperature of 94.7 °C, and crude oil properties such as a viscosity of 1.79 mPa s, a saturation pressure of 8.62 MPa, and a formation volume factor of 1.152 at 21 MPa. The gas–oil ratio is 35 under standard conditions. The CO₂ content in the associated gas remains relatively stable and high, making further CO₂ injection less effective for both enhanced oil recovery and long-term storage.

Understanding miscibility patterns during associated gas reinjection can aid in formulating onsite construction plans, whereas the mechanisms underlying miscibility between the associated gas and crude oil can provide a more comprehensive explanation for these patterns. Therefore, in this study, on the basis of the current reservoir conditions, laboratory experiments were appropriately simplified. Slim tube tests were conducted using CO₂ and associated gases with varying CO₂ concentrations to measure the minimum miscibility pressure (MMP) between crude oil and associated gases with different CO₂ concentrations. Moreover, gas injection expansion experiments were performed, and the solubilities of different injected gases in crude oil were determined to study the changes in the physical properties of the crude oil after gas injection. This study focused on the reinjection of associated gas, providing valuable reference data for field operations in oilfields.

Experimental details

Materials

In the experiment, a coiled sand-packed slim tube with a length of 15 m and a diameter of 4 mm was selected. The pore volume of the tube is 86.249 cm³ with a porosity of 45.76% and a permeability of 4860 mD. The crude oil used in the experiment was degassed oil sourced from Block H of the Jilin Oilfield, which was reconstituted into formation oil in the laboratory. The compositions of the well stream fluids and dissolved gas are listed in Table 1. The different associated gases used in the experiment were synthesized by mixing CO₂, CH₄, C₂–C₄, and liquids C₅ and C₆, with CO₂ molar ratios of 90%, 80%, 70%, and 60%, while the proportions of the other components were maintained constant. On this basis, CO₂ + CH₄ mixtures with different CO₂ molar ratios and associated gases with CH₄ and N₂ removed were also prepared. The compositions of the well stream fluids

Fluid types	Molar composition of components/%										
	N ₂	CO ₂	C ₁	C ₂	C ₃	iC ₄	nC ₄	iC ₅	nC ₅	C ₆	C ₇₊
Well fluid	1.59	0.19	17.36	3.78	2.43	0.46	1.27	0.60	1.39	3.78	67.15
Dissolved gas	6.01	0.72	66.44	13.55	7.18	0.96	2.24	0.54	0.99	1.24	0

Table 1. Composition of the well fluids and dissolved gas.

CO ₂ concentration/%	Proportions of components/%									
	N ₂	CO ₂	C ₁	C ₂	C ₃	iC ₄	nC ₄	iC ₅	nC ₅	C ₆
90	1.484	90	5.457	1.659	0.999	0.098	0.205	0.031	0.047	0.020
80	2.969	80	10.914	3.317	1.998	0.195	0.409	0.061	0.095	0.041
70	4.454	70	16.371	4.976	2.998	0.293	0.614	0.092	0.142	0.061
60	5.939	60	21.828	6.635	3.997	0.390	0.819	0.122	0.190	0.081

Table 2. Formulation data of the associated gas.

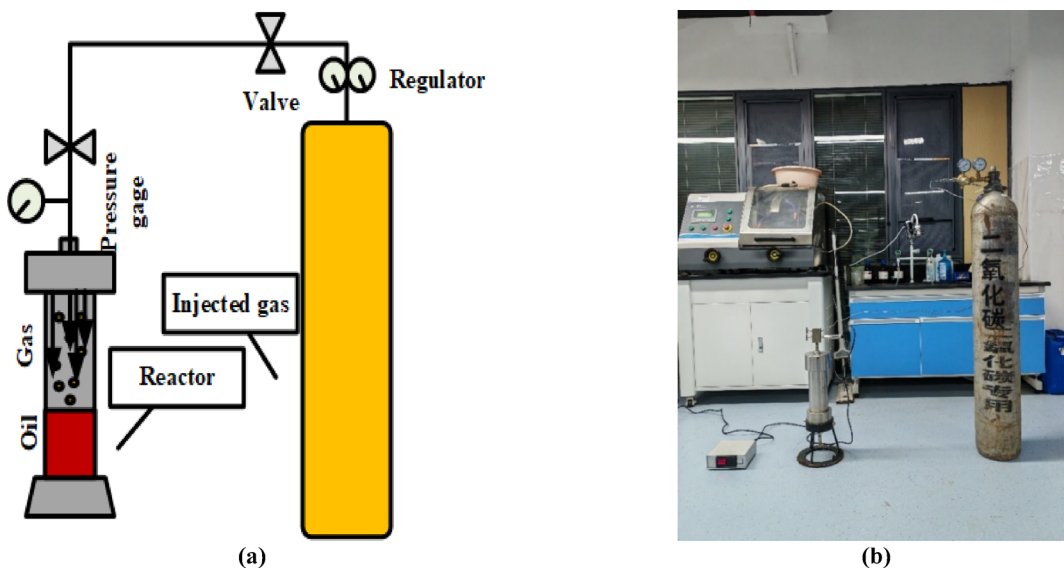


Fig. 1. Process for determining the solubilities of various gases in crude oil.

and dissolved gas are presented in Table 1, and the compositions of the associated gases with varying CO₂ concentrations are provided in Table 2.

Determination of the solubilities of different gases in crude oil

A certain mass of crude oil with an initial volume V_0 was injected into a high-temperature and high-pressure reactor. The gas to be measured was then introduced into the reactor until a certain pressure was attained. The release valve was opened to expel the air inside the apparatus. The target gas was then introduced, and once the pressure in the reactor reached the set level, the inlet was closed. The experimental temperature was set, and heating and stirring were initiated. The pressure in the reactor was recorded at 20-min intervals. Equilibrium was achieved when the recorded pressure remained constant over three consecutive readings, which is noted as the equilibrium pressure. A schematic of the experimental apparatus used is shown in Fig. 1.

The solubility of gas in crude oil can be expressed as the amount of gas (in moles) dissolved per kilogram of crude oil^{33,34}. This value can be calculated by subtracting the amount of gas remaining at equilibrium from the initial amount of injected gas:

$$X = \frac{n_0 - n_1}{m} \quad (1)$$

n_0 and n_1 can be calculated using the ideal gas equation:

$$n_0 = \frac{p_0 (V - V_0)}{Z_0 RT} \quad (2)$$

$$n_1 = \frac{p_1 (V - V_1)}{Z_1 RT} \quad (3)$$

where X is the solubility of gas in the oil (mol/kg), n_0 and n_1 are the amounts of the injected gas in the gas phase in the initial and equilibrium states, respectively (moles), m is the mass of oil (grams), p_0 and p_1 are the initial and equilibrium pressures, respectively inside the reactor (MPa),

V is the effective volume of the reactor (m³), V_0 is the volume of oil inside the reactor (m³), Z_0 and Z_1 are the compressibility factors of the injected gas in the initial and equilibrium states, respectively, R is the universal gas constant (8.314 J/mol K), and T is the temperature (Kelvin).

In the experiment, the solubilities of CO_2 , associated gas with varying CO_2 concentrations, and associated gas with CH_4 and N_2 removed in crude oil were measured under different pressure conditions at a reservoir temperature of 94.7°C .

Swelling test

The experimental setup is shown in Fig. 2. The imaging system, gas/oil supply system, PVT analyser, and temperature maintenance system are the primary components. The experimental fluids comprised formation crude oil and were contained in a sapphire observation cell with an internal diameter of 2.2 cm and a length of 40 cm. The visual cell could withstand pressures up to 50 MPa and temperatures up to 150°C in the autoclave. To investigate the effect of the injected gas on the crude oil properties and explore the miscibility mechanism, experiments were conducted at the reservoir temperature and pressure. CO_2 , associated gas with a 60% CO_2 concentration, and associated gas with a 60% CO_2 concentration after removing CH_4 and N_2 were sequentially injected into a PVT cell according to predetermined ratios³⁵. After the injection of a specific gas proportion, the pressure was gradually increased until the injected gas fully dissolved in the crude oil to form a single phase. Once each gas was injected, the high-pressure physical properties of the reservoir fluid changed. By measuring the density, bubble point pressure, expansion coefficient, and viscosity after each injection, the impact of the injected gas on the properties of the crude oil could be analysed^{36,37}. In the swelling test, all vessels were meticulously cleaned and subjected to a 2-hour vacuum evacuation. After the gauge volume and instrument pore volume were calibrated, white oil was steadily injected via an oil pump while the confining pressure was gradually increased. The system was then stabilized at a constant temperature of 94.7°C for 2 h to verify equipment integrity. Crude oil was subsequently introduced into the observation cell and maintained under equilibrium conditions for an additional 2-hour stabilization period. The experiment proceeded with stepwise injections of CO_2 and associated gas mixtures—one containing 60% CO_2 and another stripped of CH_4 and N_2 (also at 60% CO_2)—at incremental molar ratios (10%, 20%, 30%, 40%, 50% and 60%) relative to the oil initially charged into the visual cell. After gas injection, the system was pressurized with white oil, followed by 30 min of agitation to ensure complete gas

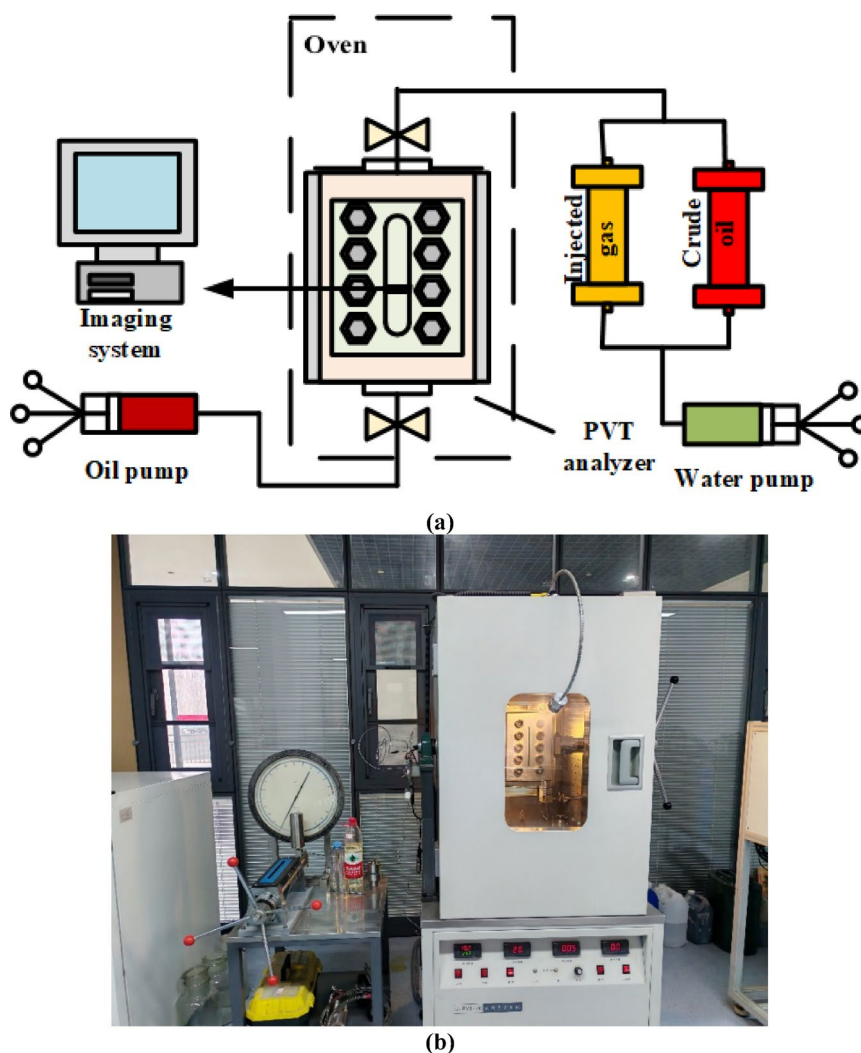


Fig. 2. Process of the swelling test.

dissolution. The density and viscosity were measured using a densitometer and viscometer, respectively. The bubble point pressure (P_b) was determined through pressure–volume (P–V) analysis by conducting a constant-composition expansion (CCE) experiment of gas-saturated crude oil (conducted in compliance with industry standard SY/T 5542-2009). The inflection point of the P–V curve corresponds to P_b ³⁸. The expansion coefficient (EC), defined as the ratio of the expanded oil volume after gas injection to the initial crude oil volume at 30 MPa, was also calculated. The entire procedure was repeated for each gas injection ratio to obtain the viscosity (μ), density, P_b , and EC of the oil sample under varying gas concentrations³⁹.

Slim tube test

In this experiment, the slim tube method was employed to measure the minimum miscibility pressure (MMP) between the injected gas and crude oil^{40,41}. Before the experiments, formation oil and gas samples were prepared according to the formulation data⁴². The experimental process is shown in Fig. 3, and the specific steps are as follows:

Cleaning the slim tube Before the experiment, the capillary tube was thoroughly cleaned to ensure readiness. After cleaning (when the colour of petroleum ether discharged from the outlet no longer changed), nitrogen gas was used to dry the tube, and a vacuum pump was applied to evacuate it.

Saturation with dead oil Under the experimental temperature and pressure conditions, the entire capillary tube was saturated with petroleum ether. The pore volume was calculated (on the basis of the difference in pump position between the start and end under constant-pressure mode). Then, dead oil (or petroleum ether) was injected to increase the system pressure to the experimental pressure.

Saturation with live oil Under the experimental temperature and pressure conditions, live oil was used to displace dead oil (2 times the pore volume). The gas–oil ratio at the capillary tube outlet was calculated. If this ratio was consistent with the gas–oil ratio of live oil, the process of saturation was complete.

Injection experiment The inlet pressure was adjusted to 0.05–0.1 MPa above the experimental pressure. Once the pump position stabilized, the initial position was recorded. Via the use of the constant-speed method, gas

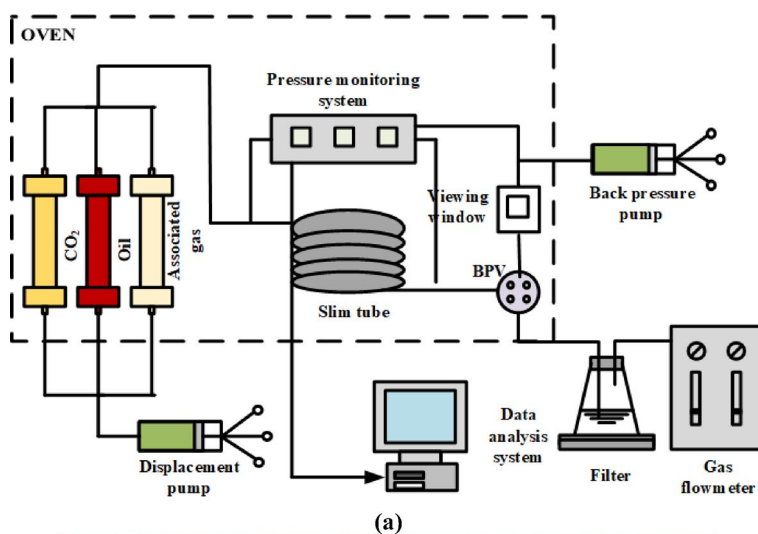


Fig. 3. Process of the slim tube test.

was injected at a speed of 0.1 cm³/min to conduct the displacement experiment. The amounts of produced oil and gas, as well as the pump position, were measured every 0.1PV. The displacement was stopped after a cumulative injection of 1.2PV.

Varying the injection pressure The injection pressure was varied while the temperature was maintained constant, and the recovery factor was determined at different injection pressures (while the PV was maintained constant at 1.2). The pressure points were determined on the basis of the recovery factor from the previous experiment, ensuring that there were at least 3 pressure points corresponding to recovery factors above and below 90%. A scatter diagram of the recovery factor versus the experimental pressure was created. Trend lines (straight lines) were generated for the two pressure ranges. The intersection of the two trend lines corresponds to the recovery factor at the MMP, and this pressure is considered the minimum miscibility pressure (MMP).

Results and discussion

Research on the miscibility mechanism of associated gas reinjection

Solubility of the injected gas in crude oil

On the basis of the experimental data and Eq. (1) to (4), the solubilities of different injected gases in crude oil under reservoir conditions were calculated. The results are listed in Table 3.

The experimental results indicated that, at a constant temperature, the solubility of gas increased with increasing initial pressure. Conversely, when the initial pressure remained constant, increasing the temperature reduced the ability of the gas to dissolve in the oil. This phenomenon suggests that increasing the injection pressure can increase gas dissolution into oil, thereby facilitating a range of effects that promote oil flow. The solubility of associated gas in oil is slightly lower than that of CO₂, whereas the removal of CH₄ and N₂ from the gas provides even greater solubility in the oil.

Analysis of the crude oil gas injection expansion experiments

Through swelling tests, the changes in the physical properties of crude oil after gas injection were analysed to study the miscibility mechanism of associated gas reinjection. After gas injection, the crude oil density minimally changed, the viscosity decreased, and both the saturation pressure and expansion coefficient increased. Figure 4 shows the experimental results.

1. Density: Although gas dissolution into crude oil reduces its density, the compression of crude oil in the pressurization process after gas injection leads to an increase in the density. Therefore, as the amount of injected gas increases, the crude oil density increases, but the maximum increase is only 0.008 g/cm³. Additionally, the injection of associated gas with N₂ and CH₄ removed performs better in reducing the crude oil density.
2. Viscosity: Gas injection leads to a significant reduction in the crude oil viscosity. The effectiveness of viscosity reduction follows the order of associated gas N₂ and CH₄ removed > CO₂ > raw associated gas. Injecting associated gas without N₂ or CH₄ decreases the viscosity from 1.79 to 0.92 mPa-s, a 48.6% reduction (Fig. 4b). This is due to CO₂ dissolving in heavy oil and in turn disrupting colloid and asphaltene structures and reducing molecular interactions. The occurrence of hydrocarbons in purified associated gas enhances this effect.
3. Saturation pressure: After gas injection, the saturation pressure of crude oil increases. CH₄ and N₂ in the associated gas inhibit gas solubility in oil, whereas hydrocarbons dissolve more readily, leading to the trends shown in Fig. 4c. After the dissolution of 51.9 m³/m³ of gas, the saturation pressures of CO₂, raw associated gas, and treated associated gas increased to 25.359, 22.733, and 19.362 MPa, respectively.
4. Expansion coefficient: The expansion coefficient reflects the extent of crude oil volume expansion due to gas dissolution during injection. As shown in Fig. 4d, the treated associated gas exhibited a greater expansion effect. Once the gas injection volume reached 51.9 m³/m³, the expansion coefficient of crude oil reached 1.39.

The experimental results indicated that after CO₂ injection, crude oil experiences volume expansion and an increase in the bubble point pressure, increasing its elastic properties in the reservoir. This finding is consistent with the analytical results of other scholars^{43,44}. Simultaneously, the viscosity decreases, enhancing oil mobility

Type of gas	Temperature (°C)	Pressure (MPa)	CO ₂ concentration (%)	Solubility (mol/kg)
CO ₂	94.7	5	100	0.138
	94.7	6	100	0.482
	60	5	100	0.186
Associated gas	94.7	5	90	0.128
			80	0.114
			70	0.104
			60	0.092
Associated gas without CH ₄ and N ₂	94.7	5	90	0.145
			80	0.243
			70	0.345
			60	0.444

Table 3. Solubility of different gases in oil.

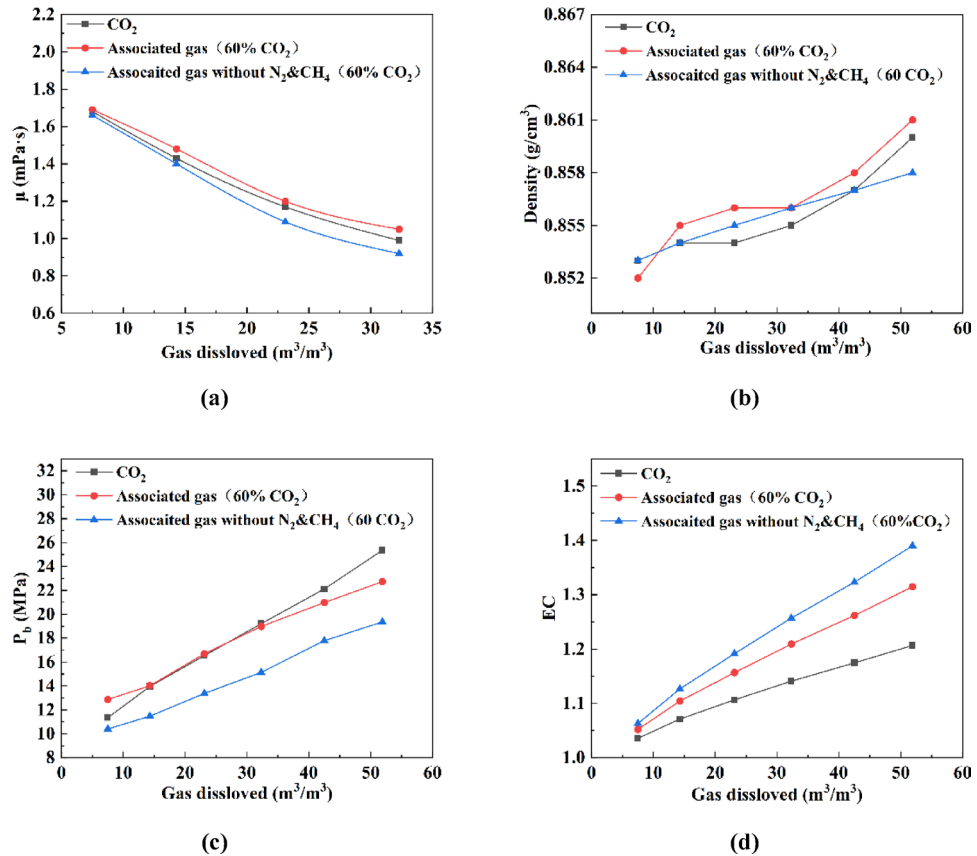


Fig. 4. **a** Relationship between the crude oil viscosity and gas injection volume, **b** relationship between the crude oil density and gas injection volume, **c** relationship between the crude oil bubble point pressure and gas injection volume, and **d** relationship between the crude oil expansion coefficient and gas injection volume.

and facilitating displacement. Compared with CO_2 alone, injecting associated gas with a 60% CO_2 content results in slightly reduced expansion and viscosity reduction effects. However, after removing N_2 and CH_4 from the associated gas, it performs even better than pure CO_2 does. In miscible or near-miscible processes, both the volumetric swelling of crude oil and the interfacial film flow substantially influence the recovery efficiency⁴⁵. An increase in the EC value significantly enhances the swelling potential of crude oil, thereby effectively reducing the minimum miscibility pressure (MMP). Experimental data from EC measurements demonstrate that increasing the gas injection volume and removing CH_4/N_2 from the injectant significantly increase crude oil expansion. These mechanisms are manifested operationally as elevated injection pressures and purified gas streams—findings that are consistent with those of prior research¹⁴.

Results of the slim tube test

Production dynamics of associated gas reinjection

In the slim tube displacement experiment, the oil and gas production rates were recorded at 0.1PV gas injection increments until 1.2PV was reached. The recovery factor and gas-oil ratio (GOR) for each stage were calculated. Figure 5 shows the GOR, stage recovery factor, MMP determination curve and immiscible state through the viewing window for associated gas with a 90% CO_2 content under various injection pressures. The results indicated that the recovery factor increases with increasing injection volume, increasing rapidly before 0.9PV. During the early injection phase (before 0.4PV), lower injection pressures yield faster growth, with a growth rate of approximately 9.3% per 0.1PV at 21 MPa. The GOR under each injection pressure significantly increased after 0.9PV, reaching its peak at 1.2PV. Similar production patterns were observed for associated gases with different CO_2 concentrations.

The analysis of the experimental results indicated that, prior to breakthrough, the recovery factor during associated gas flooding increases rapidly with increasing injection volume. This effect is especially pronounced at lower injection pressures, where recovery increases more quickly at the early stages. This occurs because, when the injection pressure is below the MMP, CO_2 can hardly be mixed with crude oil, and the displacement process resembles immiscible displacement. However, lower injection pressures lead to lower recovery rates at the later stages. The main reason is that CO_2 creates preferential flow channels after pore oil is displaced, causing most of the injected CO_2 to flow along these channels, which results in a sharp increase in the gas-oil ratio⁴⁶. Consequently, the oil in other pore spaces is less likely to be displaced by CO_2 , leading to a lower ultimate recovery at low injection pressures⁴⁷.

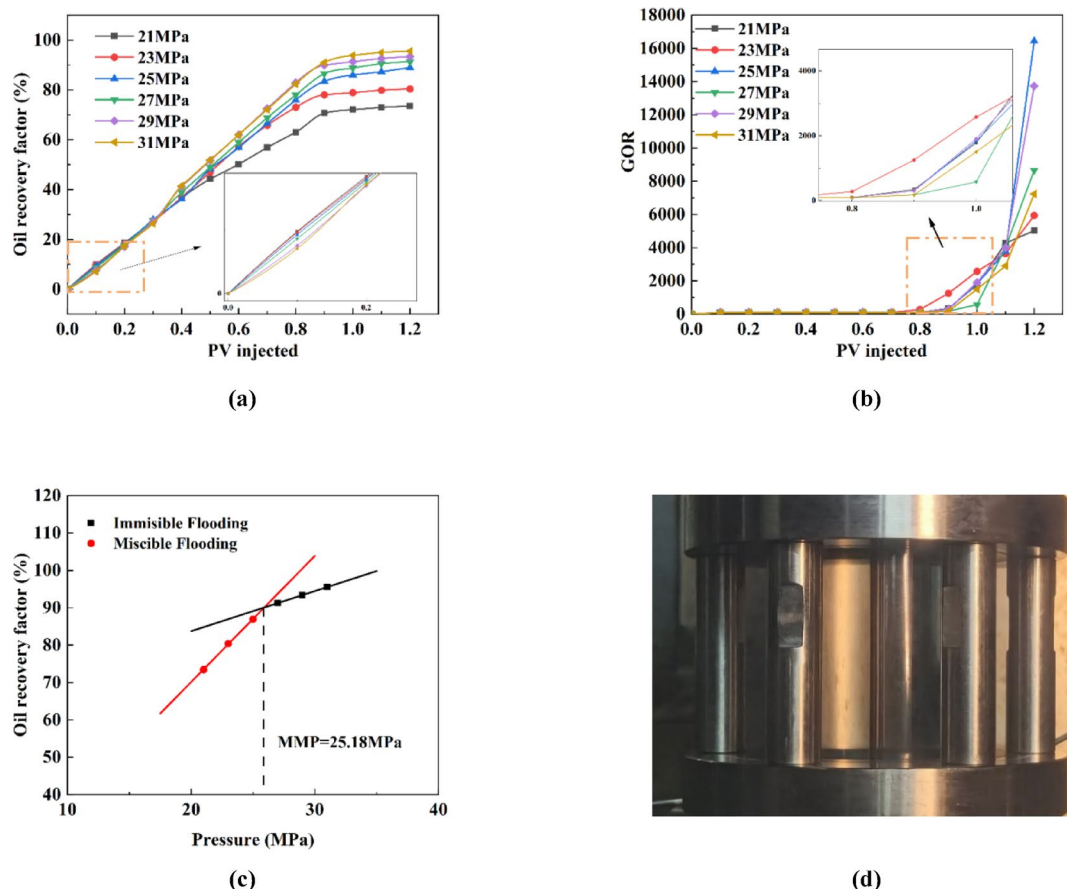


Fig. 5. Production patterns of associated gas with a 90% CO_2 concentration under different injection pressures and MMP determination curves: **a** incremental recovery factor, **b** production gas-oil ratio (GOR), **c** MMP determination curve and, **d** immiscible state.

Influence of associated gas reinjection on the minimum miscibility pressure

Exploring the influence of associated gas reinjection on the minimum miscibility pressure (MMP), as well as the mechanisms by which each component of the associated gas affects the MMP, is valuable for predicting field recovery rates. Via the use of the slim tube method, the MMPs of associated gases with varying CO_2 contents, $\text{CO}_2 + \text{CH}_4$ mixtures, and associated gases with CH_4 and N_2 removed with crude oil were determined. The corresponding trends in the MMP with changes in the injected gas composition were analysed.

The relationship curve between the MMP and CO_2 concentration in the gas injected into crude oil is shown in Fig. 6. The results indicated that the MMP exhibits a notable linear correlation with the CO_2 concentration in the injected gas, with correlation coefficients above 0.97. When CH_4 is present in the injected gas, the MMP increases as the CO_2 content decreases. For every 10% decrease in the CO_2 concentration in the associated gas, the MMP increases by 0.937 MPa, reaching 27.94 MPa when the CO_2 concentration is relatively low (60%). The MMP of the $\text{CO}_2 + \text{CH}_4$ mixture increases even more rapidly, with a 3.07 MPa higher pressure than that of the associated gas with a 60% CO_2 concentration. Conversely, the MMP behaviour of the associated gas without CH_4 and N_2 indicated a different trend, with the MMP decreasing by 2.469 MPa for every 10% reduction in the CO_2 concentration. This modified associated gas remains miscible with crude oil even at low CO_2 concentrations, achieving an MMP of only 14.53 MPa at a 60% CO_2 level.

Gas miscible displacement operates through two principal mechanisms: condensing and vaporizing gas drive processes. In the vaporizing gas drive process, which typically involves CO_2 , N_2 , and CH_4 in the associated gas, the injected gas strips light and intermediate components from the crude oil, thereby gradually enriching the gas phase to attain miscibility. Conversely, in the condensing gas drive process, which primarily occurs in the presence of abundant gas components ($\text{C}_2 - \text{C}_6$), the gas condenses into the crude oil, thereby enriching the oil phase to achieve miscibility. Notably, achieving miscibility with lean gases such as CH_4 and N_2 poses greater challenges because of their limited capacity for enrichment compared with that of heavier hydrocarbons⁴⁸. The analysis of the associated gas composition reveals that methane is the dominant constituent, with the vaporizing gas drive process serving as the primary mechanism for miscible flooding. As the CO_2 concentration in the associated gas increases, the relative methane content decreases, thereby enhancing the extraction capacity of the gas phase for light hydrocarbon fractions from crude oil. This phenomenon results in a corresponding reduction in the minimum miscibility pressure (MMP) with increasing CO_2 content. Removing CH_4 and N_2 effectively reduces the MMP. When these gases are removed from the associated gas, the remaining components, apart

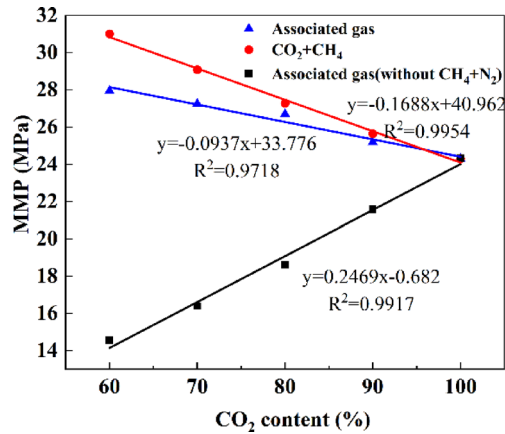


Fig. 6. Relationship curves between the MMP of different gas-oil injection systems and the CO₂ concentration in the injection gas.

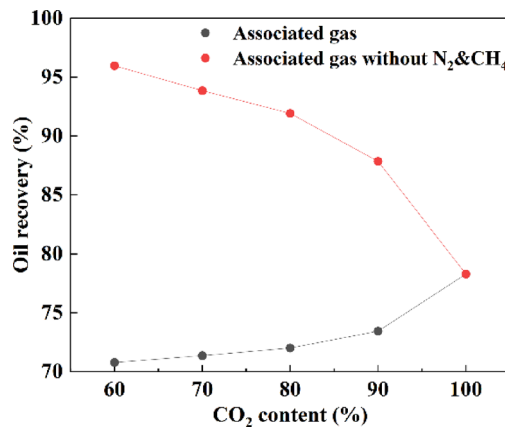


Fig. 7. Displacement efficiency of CO₂ and associated gas with respect to the reservoir pressure.

from CO₂, are light fractions of crude oil. Consequently, the dominant mechanism for miscibility achievement shifts to the condensing gas drive process. The resulting MMP becomes dependent on the concentration of enriched hydrocarbon fractions (C₂–C₆) in the purified gas stream. This explains the observed phenomenon in which the MMP paradoxically increases with increasing CO₂ content.

Notably, the injection of enriched gas provides superior displacement efficiency, yielding lower MMP values than the reinjection of unprocessed associated gas does, as observed in relevant studies²⁵. This results in the curve being lower than the curve for associated gas reinjection^{49,50}. Notably, the asphaltene content in crude oil also significantly impacts the MMP. The MMP increases linearly with increasing asphaltene concentration^{38,51,52}. In this study, conventional black oil was employed as the sample. However, when analysing heavy oil, injecting purified associated gas may yield a larger reduction in the miscibility pressure.

Oil displacement efficiency of associated gas

To evaluate the oil displacement capacity of the associated gas, the recovery factor was calculated after injecting associated gases with different CO₂ concentrations up to 1.2PV into a slim tube at reservoir pressure (21 MPa) and compared with that of pure CO₂ injection under the same conditions. The results are shown in Fig. 7. At the current reservoir pressure, which is significantly lower than the CO₂–oil MMP, the efficiency of CO₂ flooding is less than 90%. The oil displacement efficiency of associated gas reinjection is lower than that of pure CO₂, and at the reservoir pressure, the lower the CO₂ concentration in the associated gas is, the lower the displacement efficiency. With an associated gas containing 60% CO₂, the displacement efficiency decreased by 7.92% compared with that with pure CO₂.

The low oil displacement efficiency of associated gas is due mainly to the presence of CH₄ and N₂, which reduces the oil displacement efficiency of the direct reinjection of associated gas compared with that of the injection of purified associated gas (with CH₄ and N₂ removed). The comparison revealed a significant increase in the oil displacement efficiency after CH₄ and N₂ were removed, resulting in a nearly miscible displacement state. When the CO₂ concentration reaches 90%, the displacement efficiency increases by 14.39%. As the displacement efficiency of associated gas is positively correlated with the CO₂ concentration, while the injection

of purified associated gas exhibits an inverse relationship, removing CH₄ and N₂ can achieve greater efficiency improvement at lower CO₂ concentrations. For example, at a 60% CO₂ concentration, the oil displacement efficiency of purified associated gas increases by 25.59%.

It is undeniable that purifying CH₄ and N₂ also incurs costs⁵³. Therefore, while aiming to increase recovery rates, a balance should be maintained between the investment costs and benefits. Achieving effective CO₂ sequestration while maximizing profitability will be a critical focus of future research.

Conclusion

1. Both lowering the temperature and increasing the pressure enhance the dissolution of CO₂ into crude oil. Compared with CO₂, associated gas is less soluble in crude oil. Under conditions of 94.7 °C and 5 MPa, the solubility of CO₂ in crude oil is 1.07 to 1.5 times greater than that of associated gas. Removing CH₄ and N₂ significantly enhances the solubility of associated gas, yielding a 1.05 to 3.22 times greater solubility than that of CO₂. The injection of CO₂ or associated gas can reduce the crude oil viscosity and increase the expansion energy of fluids in the reservoir. This effect increases with increasing gas solubility. Therefore, CO₂ flooding or associated gas injection can increase oil recovery through the optimization of the composition of the injected gas or the incorporation of solubility-enhancing agents.
2. The CO₂ concentration in the associated gas influences the minimum miscibility pressure (MMP): for every 10% decrease in the CO₂ concentration, the MMP increases by 0.937 MPa. Methane (CH₄) increases the MMP, with each 10% increase in CH₄ in the CO₂-CH₄ mixture resulting in an increase in the MMP of 1.688 MPa. Removing CH₄ and nitrogen (N₂) from the associated gas effectively reduces the MMP, with reductions varying between 14.4% and 48.0%. Under the current reservoir pressure, pure CO₂ injection cannot achieve miscible displacement, and the oil recovery efficiency of associated gas reinjection is even lower than that of pure CO₂ injection. This efficiency gap increases as the CO₂ concentration decreases, with a 7.92% reduction in the recovery efficiency when associated gas with a 60% CO₂ concentration is used compared with that when using pure CO₂. Removing CH₄ and N₂ from associated gas enhances the oil recovery efficiency, especially at lower CO₂ concentrations; for example, associated gas with a 60% CO₂ concentration and without CH₄ and N₂ achieves a 25.59% increase in the recovery efficiency.
3. The composition of the injected gas significantly impacts the minimum miscibility pressure (MMP). During the reinjection of associated gas in oilfields, the removal of CH₄ and N₂ through physical or chemical treatment can increase both the economic efficiency and environmental sustainability. This study highlights the need for further research to optimize the cost-benefit balance in engineering operations while ensuring rigorous health, safety, and environmental (HSE) management.

Data availability

The authors declare that all the data generated or analysed in this study are included in this published article.

Received: 27 February 2025; Accepted: 5 August 2025

Published online: 19 August 2025

References

1. Wang, H., Tian, L., Chai, X., Wang, J. & Zhang, K. Effect of pore structure on recovery of CO₂ miscible flooding efficiency in low permeability reservoirs. *J. Pet. Sci. Eng.* **208**, 109305 (2022).
2. Vafaie, A., Cama, J., Soler, J. M., Kivi, I. R. & Vilarrasa, V. Chemo-hydro-mechanical effects of CO₂ injection on reservoir and seal rocks: a review on laboratory experiments. *Renew. Sustain. Energy Rev.* **178**, 113270 (2023).
3. Zhang, Z. et al. Experimental study on the influencing factors and pore production law of CO₂ huff-and-puff in tight sandstone reservoirs. *Sci. Rep.* **15**, 3492 (2025).
4. Bashir, A. et al. Comprehensive review of CO₂ geological storage: exploring principles, mechanisms, and prospects. *Earth Sci. Rev.* **249**, 104672 (2024).
5. Jalili Darbandi Sofla, M., Farahani, D., Ghorbanizadeh, Z., Namdar, H. & S. & Experimental study of asphaltene deposition during CO₂ and flue gas injection EOR methods employing a long core. *Sci. Rep.* **14**, 3772 (2024).
6. Gbadamosi, A. O., Kiwalabye, J., Junin, R. & Augustine, A. A review of gas enhanced oil recovery schemes used in the North sea. *J. Pet. Explor. Prod. Technol.* **8**, 1373–1387 (2018).
7. Emam, E. A. Gas flaring in industry: an overview. *Pet. Coal* **57**, 532–555 (2015).
8. Elvidge, C. D. et al. The potential role of natural gas flaring in meeting greenhouse gas mitigation targets. *Energy Strategy Rev.* **20**, 156–162 (2018).
9. Khalili-Garakani, A., Iravaninia, M. & Nezhadfar, M. A review on the potentials of flare gas recovery applications in Iran. *J. Clean. Prod.* **279**, 123345 (2021).
10. Brown, K. et al. The history and development of the IEA GHG Weyburn-Midale CO₂ monitoring and storage project in saskatchewan, Canada (the world largest CO₂ for EOR and CCS program). *Petroleum* **3**, 3–9 (2017).
11. Jensen, G. K. Weyburn oilfield core assessment investigating cores from pre and post CO₂ injection: determining the impact of CO₂ on the reservoir. *Int. J. Greenhouse Gas Control.* **54**, 490–498 (2016).
12. Belmabkhout, Y. et al. Natural gas upgrading using a fluorinated MOF with tuned H₂S and CO₂ adsorption selectivity. *Nat. Energy.* **3**, 1059–1066 (2018).
13. Su, K., Liao, X., Zhao, X. & Zhang, H. Coupled CO₂ enhanced oil recovery and sequestration in china's demonstration project: case study and parameter optimization. *Energy Fuels.* **27**, 378–386 (2013).
14. Yang, S. L. et al. Mechanism of produced gas reinjection during CO₂ flooding by chromatographic analysis. *J. Dispers. Sci. Technol.* **34**, 342–346 (2013).
15. Kaya, E. & Zarrouk, S. J. Reinjection of greenhouse gases into geothermal reservoirs. *Int. J. Greenhouse Gas Control.* **67**, 111–129 (2017).
16. Mungan, N. Canada—World leader in hydrocarbon miscible flooding. *J. Can. Pet. Technol.* **41**, 35–37 (2002).
17. Wasylchuk, G. Co-injection EOR technology increases recovery and reduces GHG emissions. in (OnePetro, 2024). <https://doi.org/10.2118/218653-MS>

18. Glanville, P., Fridlyand, A. & Yan Z. From town gas to hydrogen: historical and modern perspectives on transitions between delivered fuels in the built environment. *ASHRAE Trans.* **129**, 92–102 (2023).
19. Akervoll, I., Talukdar, M. S., Midtlyng, S. H., Stensen, J. A. & Torsaeter, O. WAG Injection Experiments With In-Situ Saturation Measurements at Reservoir Conditions and Simulations. inOnePetro. <https://doi.org/10.2118/59323-MS> (2000).
20. Carpenter, A. Oil pollution in the North sea: the impact of governance measures on oil pollution over several decades. *Hydrobiologia* **845**, 109–127 (2019).
21. Gunawan, S., Caié, D. H. & Field Three years of Lean-Gas injection into waterflooded reservoirs. *SPE Reserv. Eval. Eng.* **4**, 107–113 (2001).
22. Chen, S. M., Allard, D. R. & Anli, J. Factors affecting solvent slug size requirements In hydrocarbon miscible flooding. In (OnePetro, 1984). <https://doi.org/10.2118/12636-MS>
23. Glasø, Ø. Generalized minimum miscibility pressure correlation. *Soc. Pet. Eng. J.* **25**, 927–934 (1985).
24. Shyeh-Yung, J. J. & Stadler, M. P. Effect of injectant composition and pressure on displacement of oil by enriched hydrocarbon gases. *SPE. Reserv. Eng.* **10**, 109–115 (1995).
25. Hoffman, B. T. Comparison of Various Gases for Enhanced Recovery from Shale Oil Reservoirs. inOnePetro. <https://doi.org/10.2118/154329-MS> (2012).
26. Wan, T., Sheng, J. J. & Soliman, M. Y. Evaluation of the EOR Potential in Shale Oil Reservoirs by Cyclic Gas Injection. inOnePetro, (2013).
27. Akbarabadi, M., Alizadeh, A. H., Piri, M. & Nagarajan, N. Experimental evaluation of enhanced oil recovery in unconventional reservoirs using cyclic hydrocarbon gas injection. *Fuel* **331**, 125676 (2023).
28. Aoun, A. E. et al. Enhanced oil recovery through alternating gas re-injection to reduce gas flaring in the Bakken. *Energy* **290**, 130103 (2024).
29. Sancet, G. F. et al. Compositional and numerical modeling of the HnP technique by using both dry and rich gas to increase production and reserves in shale oil wells in Vaca Muerta. in *Latin America Unconventional Resources Technology Conference, 46 December 268–305* (Unconventional Resources Technology Conference (URTeC), 2024). 268–305 (Unconventional Resources Technology Conference (URTeC), 2024). (2023). <https://doi.org/10.15530/urtec-2023-3967547>
30. Pospisil, G. et al. Report on the first rich gas EOR Cyclic multiwell Huff N puff pilot In the Bakken tight oil play. In (OnePetro, 2020). <https://doi.org/10.2118/201471-MS>
31. Grinestaff, G. et al. OnePetro.. Evaluation of eagle ford cyclic gas injection EOR: field results and economics (2020). <https://doi.org/10.2118/200427-MS>
32. Baillie, J. et al. Methane emissions from conventional and unconventional oil and gas production sites in southeastern saskatchewan, Canada. *Environ. Res. Commun.* **1**, 011003 (2019).
33. Kavousi, A., Torabi, F. & Chan, C. Experimental measurement of CO₂ solubility In heavy oil and its diffusion coefficient calculation at both static and dynamic conditions. In (OnePetro, 2013). <https://doi.org/10.2118/165559-MS>
34. Mosavat, N. & Torabi, F. Performance of secondary carbonated water injection in light oil systems. *Ind. Eng. Chem. Res.* **53**, 1262–1273 (2014).
35. Abedini, A., Mosavat, N. & Torabi, F. Determination of minimum miscibility pressure of crude oil–CO₂ system by oil swelling/extraction test. *Energy Technol.* **2**, 431–439 (2014).
36. Fakher, S., Elgahawy, Y. & Abdelaal, H. Oil Swelling Measurement Techniques: Conventional Methods and Novel Pressure-Based Method. inOnePetro, (2020). <https://doi.org/10.15530/urtec-2020-1073>
37. Gandomkar, A., Nasriani, R., Enick, H., Torabi, F. & R. M. & The effect of CO₂-philic thickeners on gravity drainage mechanism in gas invaded zone. *Fuel* **331**, 125760 (2023).
38. Potsch, K., Toplack, P. & Gumpfenberger, T. A review and extension of existing consistency tests for PVT data from a laboratory. *SPE Reserv. Eval. Eng.* **20**, 269–284 (2017).
39. Lobanov, A. A. et al. Swelling/extraction test of Russian reservoir heavy oil by liquid carbon dioxide. *Pet. Explor. Dev.* **45**, 918–926 (2018).
40. Zhang, K. & Gu, Y. Two different technical criteria for determining the minimum miscibility pressures (MMPs) from the slim-tube and coreflood tests. *Fuel* **161**, 146–156 (2015).
41. Voon, C. L. & Awang, M. Comparison of MMP between slim tube test and vanishing interfacial tension test. in ICIPPEG 2014 (eds Awang, M., Negash, B. M., Akhir, M. & Lubis, L. A.) N. A. 137–144 (Springer, Singapore, doi:https://doi.org/10.1007/978-981-287-368-2_13). (2015).
42. Su, Y. et al. The influence of slim tube length on the minimum miscibility pressure of CO₂ gas–crude oil. *Processes* **12**, 650 (2024).
43. Arouri, K. R. & Herrera, C. G. Phase envelopes in reservoir fill analysis: two contrasting scenarios. *Sci. Rep.* **14**, 5601 (2024).
44. Guo, X. et al. SPE, Tulsa, Oklahoma, USA., Optimization of tertiary water-alternate-CO₂ flood in jilin oil field of China: laboratory and simulation studies. in *SPE/DOE Symposium on Improved Oil Recovery* SPE-99616-MS (2006). <https://doi.org/10.2118/99616-MS>
45. Ghorbani, M., Gandomkar, A. & Montazeri, G. Describing a strategy to estimate the CO₂-heavy oil minimum miscibility pressure based on the experimental methods. *Energy Sour. Part A Recover. Util. Environ. Eff.* **41**, 2083–2093 (2019).
46. Zhou, X. et al. Performance evaluation of CO₂ flooding process in tight oil reservoir via experimental and numerical simulation studies. *Fuel* **236**, 730–746 (2019).
47. Adel, I. A., Tovar, F. D., Schechter, D. S. & Fast-Slim Tube A reliable and rapid technique for the laboratory determination of MMP In CO₂—Light crude oil systems. In (OnePetro, (2016). <https://doi.org/10.2118/179673-MS>
48. Stalkup, F. I. Displacement behavior of the condensing/vaporizing gas drive process. In (OnePetro, 1987). <https://doi.org/10.2118/16715-MS>
49. Keyvani, F., Safaei, A., Kazemzadeh, Y., Riazi, M. & Qajar, J. Impact of nanopore confinement on phase behavior and enriched gas minimum miscibility pressure in asphaltenic tight oil reservoirs. *Sci. Rep.* **14**, 13405 (2024).
50. Fomkin, A. V., Petrakov, A. M., Nikitina, E. A. & Egorov, Y. A. Features of filtration experiments studying oil displacement by gas on slim tube as a reservoir model (Russian). *Neftyanoe khozyaystvo Oil Ind.* **2023**, 42–45 (2023).
51. Ghorbani, M. et al. Experimental investigation of asphaltene content effect on crude Oil/CO₂ minimum miscibility pressure. *Period Polytech. Chem. Eng.* **64**, 479–490 (2020).
52. Torabi, F. & Gandomkar, A. Experimental evaluation of CO₂-soluble nonionic surfactants for wettability alteration to intermediate CO₂-oil wet during immiscible gas injection. *SPE J.* **29**, 5071–5086 (2024).
53. Shen, M. et al. Cryogenic technology progress for CO₂ capture under carbon neutrality goals: a review. *Sep. Purif. Technol.* **299**, 121734 (2022).

Acknowledgements

This work is supported by the National Natural Science Foundation of China (No. 51404037) “Solubility Behavior of High-Temperature, High-Pressure CO₂-Oil-Formation Water Three-Phase Equilibrium” and the National Natural Science Foundation of China (No. 52104022) “Mechanism of supercritical CO₂ composite flooding to enhance gas recovery in tight gas reservoirs under the influence of water shield”.

Author contributions

Yunfei Lei: Conceptualization, visualization, writing—original draft, data curation, experimental execution, and formal analysis. Changquan Wang: Methodology, data curation, writing—original draft, project administration, resources, and writing—review and editing. Shijin Xu: Investigation, supervision, and writing—review and editing. Lihong Shi: Supervision and writing—review and editing. Xinke Jin: Formal analysis, experimental execution, and investigation. Weijie Fu: Reviewing and editing.

Declarations

Competing interests

The authors declare no competing interests.

Additional information

Correspondence and requests for materials should be addressed to C.W.

Reprints and permissions information is available at www.nature.com/reprints.

Publisher's note Springer Nature remains neutral with regard to jurisdictional claims in published maps and institutional affiliations.

Open Access This article is licensed under a Creative Commons Attribution-NonCommercial-NoDerivatives 4.0 International License, which permits any non-commercial use, sharing, distribution and reproduction in any medium or format, as long as you give appropriate credit to the original author(s) and the source, provide a link to the Creative Commons licence, and indicate if you modified the licensed material. You do not have permission under this licence to share adapted material derived from this article or parts of it. The images or other third party material in this article are included in the article's Creative Commons licence, unless indicated otherwise in a credit line to the material. If material is not included in the article's Creative Commons licence and your intended use is not permitted by statutory regulation or exceeds the permitted use, you will need to obtain permission directly from the copyright holder. To view a copy of this licence, visit <http://creativecommons.org/licenses/by-nc-nd/4.0/>.

© The Author(s) 2025